

1 Article's Supplementary Materials

2 **Supplementary Materials: The Effect of Annealing Temperature on ECD Grown Hexagonal-**
 3 **Plane Zinc Oxide**

4 **Sukrit Sucharitakul¹, Rangsan Panyathip¹ and Supab Choopun^{1,*}**

5 ¹ 1 Department of Physics and Materials, Faculty of Science, Chiang Mai University, 239 Huay
 6 Keaw Road, Muang Chiang Mai, 50200, Thailand

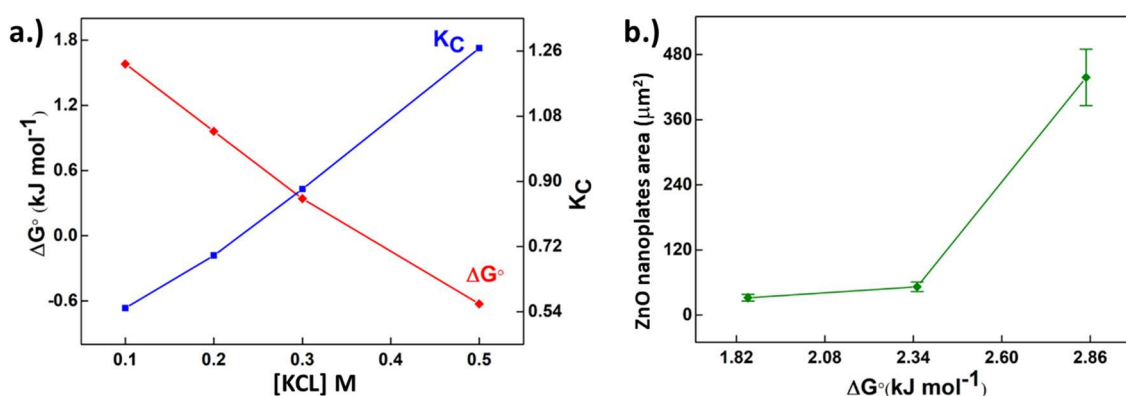
7 * Correspondence: supab99@gmail.com; Tel.: +66-819-512-669

8 Academic Editor: <>

9 Received: <>; Accepted: <>; Published: <>

10

11 **SI: The effect of KCl Concentration on Growth Parameters**



12

13 Figure. S1 Plot of calculated a.) the reaction rate in equilibrium K_C and the variable of Gibbs free

14 energy level (ΔG°) versus KCl concentration and b.) the h-ZnO's nanoplatelet sizes' plotted with ΔG°

15

16 This section of supplementary materials discusses the role of KCl and annealing temperature
 17 in h-ZnO growths. As shown in Figure S1.a.), the relativity of thermodynamic equilibrium constant
 18 (K_C) was calculated via equation (2) and plotted versus the concentration of KCl in our experimental
 19 range (0.1M-0.5M) to gain further insights on its effects on the growth of h-ZnO. In this investigation,
 20 the concentration of KCl is used as primary variable to figure out other parameters. K_C is then
 21 calculated to determine the reaction rate in equilibrium based on the final concentration. As for the
 22 results, ZnO grown from 0.1M, 0.2M and 0.3M had reaction rate at 0.55, 0.6955 and 0.879 respectively.
 23 Since all K_C were determined to be less than unity, it means the reaction remains sub-equilibrium
 24 while in 0.5M case the K_C was determined to be 1.2678, whilst, this behavior is consistent with CV
 25 results from earlier.



27
$$K_C = \frac{[\text{ZnCl}_2][\text{KNO}_3]^2}{[\text{Zn}(\text{NO}_3)_2][\text{KCl}]^2} \quad (\text{SI2})$$

28 Typically, in growing homogeneous and large flakes, it's more preferable to stay well under
 29 equilibrium kinetically so that the thermodynamic can have sufficient time to kick in to the reaction,

30 which will be discussed in the next section of the supplementary materials, and such is why 0.1M of
31 KCl was determined to be optimal for growing (0001) ZnO crystal in our case.

32 When discussing thermodynamics of the h-ZnO crystal growths, Gibbs free energy of the
33 reaction in equilibrium (ΔG°) can be used to determine the favorability of nucleation in h-ZnO with
34 an electrochemical process which it defined the lowest energy to excited for reaction. This Gibbs free
35 energy term was implicated with the reaction rate constant shown in equation (3):

$$36 \quad \Delta G^\circ = -RT \ln K_c \quad (\text{SI3})$$

37 Where R is gas constant J mol^{-1} and temperature (T) The considered ΔG° in equilibrium system
38 contributed to mechanism or nucleation of ZnO in solution as equation (4) which this relation was
39 included ΔG° of nucleation surface ($\Delta G_{\text{surface}}$) and ΔG° of nucleation volume.

40 In order to determine the spontaneity of the reaction, ΔG° was calculated using equation (SI3)
41 through the calculated K_c values of the corresponding case as shown in Figure SI1. Based on our
42 results at 0.5M of KCl ΔG° is $-0.627 \text{ kJ mol}^{-1}$ making the reaction spontaneous while for 0.1M, 0.2M and
43 0.3M of KCl composition had ΔG° for 1.58 kJ mol^{-1} , 0.96 kJ mol^{-1} and 0.34 kJ mol^{-1} respectively (as
44 shown in Figure S1). Moreover, since in 0.1M -0.3M cases, $\Delta G^\circ > 0$, this reaction required another
45 parameter to excitation process with either applied voltage or annealing temperature. Furthermore,
46 based on our growths and annealing of h-ZnO flakes at different conditions shown in Figure 4.f.),
47 presented in Figure SI2 is the calculated ΔG° for each flake sizes via equation (3).

48

49 Generally, nucleation atom was assumed to sphere shape, therefore, ΔG° in nucleation atom
50 in ZnO as defined in equation (5)

$$51 \quad \Delta G^\circ = \Delta G_{\text{surface}} + \Delta G_{\text{volume}} \quad (\text{SI4})$$

52

$$53 \quad \Delta G^\circ = 4\pi(r^*)^2\gamma + \frac{4}{3}\pi(r^*)^3\Delta G_v \quad (\text{SI5})$$

54

$$55 \quad r^* = \frac{-2\gamma}{\Delta G_v} \quad (\text{SI6})$$

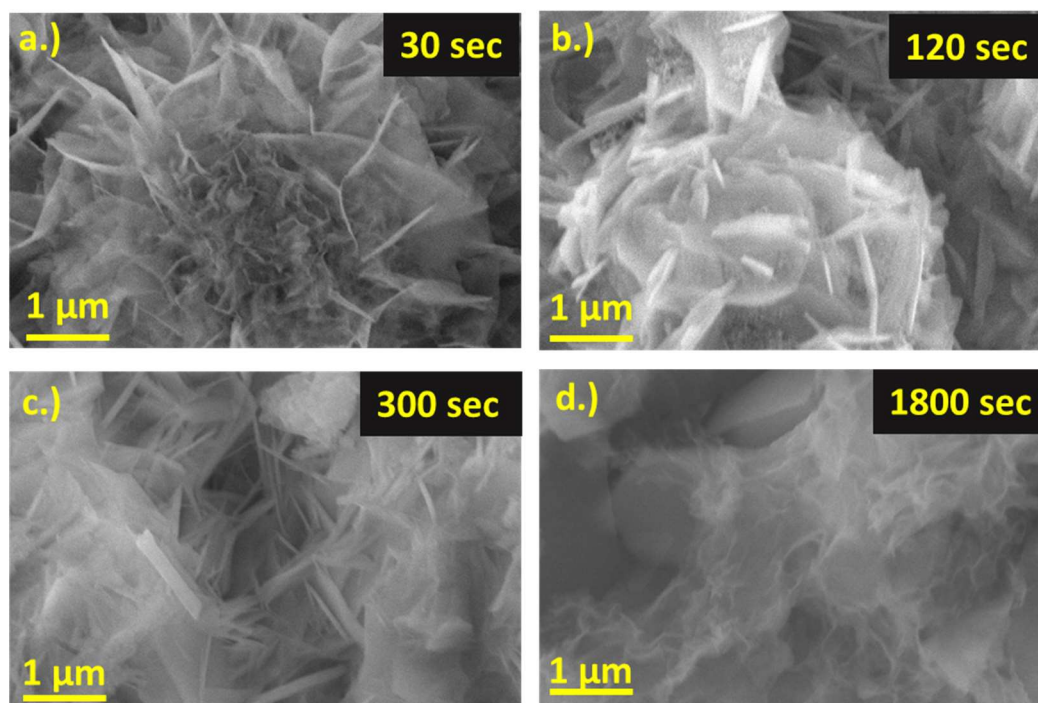
56 Where γ is the surface area of the nucleating atom, the ΔG_v is the term of the free energy of the
57 bulk crystal and r^* is the critical radian of nucleation as shown in equation (6).

58 ΔG° in nucleation mechanism has the direct proportionality with radian of nucleation (r) e.g.
59 the nucleation radian was extended as the ΔG° increases. Another parameter is r^* which is strongly
60 correlated to the size of atomic nucleation to the bulk crystal. Generally, the r has direct change with
61 $\Delta G_{\text{surface}}$ and the maximum of $\Delta G_{\text{surface}}$ is r^* point which this point showed the highest of $\Delta G_{\text{surface}}$
62 and on the other hand the ΔG_{volume} has indirect change with r extended consequently, ΔG° in this
63 mechanism was combined with $\Delta G_{\text{surface}}$ and ΔG_{volume} which the saturated point of both
64 parameters is r^* point (r_{critic} of Figure 7 (c) from Choopun *et al*, 2010¹) that meaning at r^* is the stable
65 state of nucleation atom (highest of $\Delta G_{\text{surface}}$ and lowest of ΔG_{volume}) and ready to grow for bulk
66 crystal.

$$67 \quad \Delta G^\circ = \Delta G_{\text{surface}} + \Delta G_{\text{volume}} \quad (\text{SI7})$$

68 Therefore, this growth mechanism favored r^* in determining the probability of the bulk
69 crystal grown. When $r > r^*$ the nucleation atom can perform to bulk crystal, however, if $r < r^*$ the
70 nucleation of bulk crystal is considered thermodynamically less preferred. ¹⁻⁶.

71



72

73 Figure.S2 SEM image of grown h-ZnO flakes on the electrode at a.)30 seconds, b.) 120 seconds, c.) 300
74 seconds and d.) 1800 seconds into the growth.

75

76 In conclusion, the two-step of h-ZnO flakes growth were determined with reaction rate via
77 electron transfer of electrode surface and electrolyte in primary growth process which the low
78 reaction rate as 0.1M of KCl was the reasonable condition to nucleation ZnO crystal after that using
79 secondary growth was the coalescence effect to fusion nucleation grains of ZnO in primary growth
80 for the improved and relatively larger h-ZnO flakes' size in this work.

81

82

83

84

85

86

87

88

89

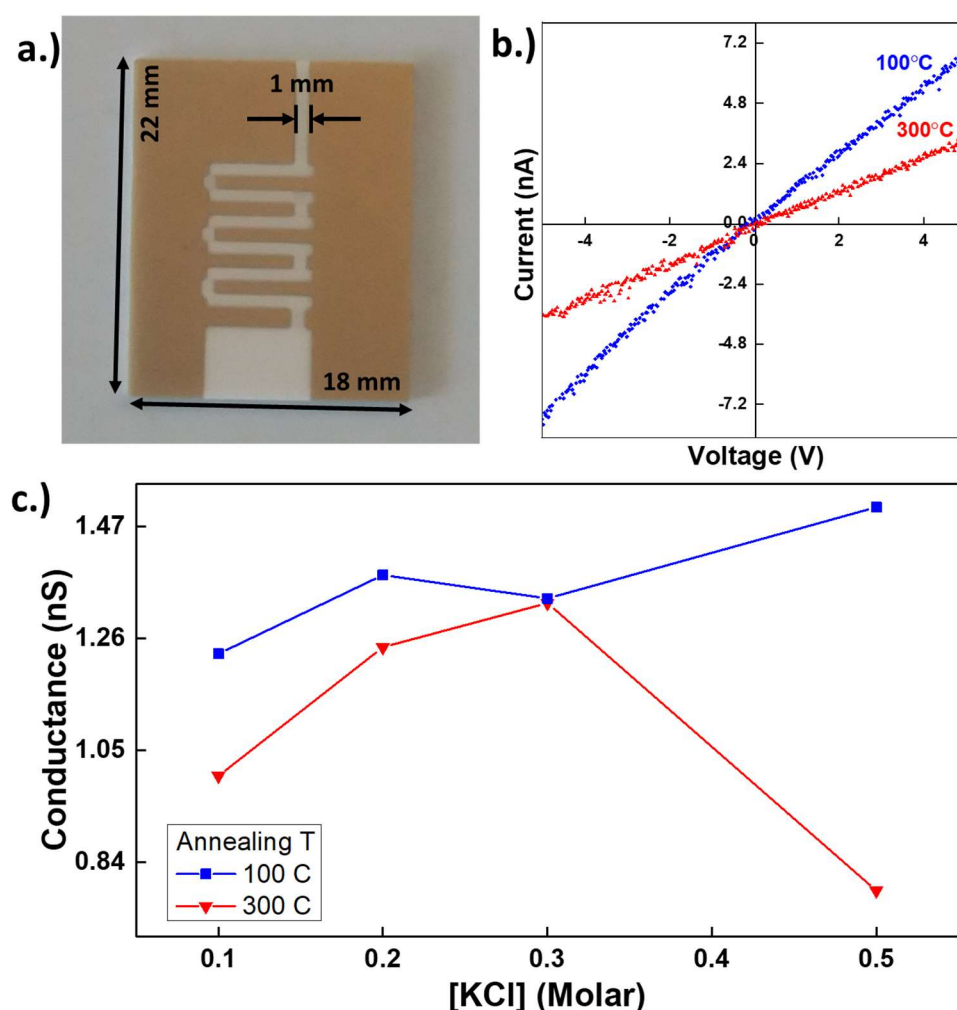
90

91

92

93

94 SII: ZnO electrical measurements



95

96 Figure S3. Illustration of a.) the device fabricated for deposited ZnO flakes, b.) I-V curve of the ZnO
 97 nanoflakes device with [KCl] = 0.5 M and c.) the calculated conductance of ZnO device vs [KCl] used
 98 in the synthesis.

99

100 To further demonstrate the capability of the grown material for applications for our proposed
 101 growth method, ZnO electrical measurements were conducted. The alumina substrate was
 102 lithographed with Au deposition as demonstrated in Figure S3.a.) prior to ZnO deposition via sol-
 103 gel process on the prepared substrate. A series of I-V test was conducted on samples annealed at 100
 104 and 300 °C while prepared from various KCl concentration for comparison. The example of our I-V
 105 result is shown in Figure S3.b.) where the device demonstrate linear contact with Au. This
 106 demonstrates the effectiveness of ZnO prepared via this method as electron collection layer for
 107 temperature sensitive Perovskites ⁷. From extracted conductance in Figure S3.c.), it is very notable
 108 that devices made of flakes annealed at 100 °C has higher conductance compared to the 300 °C ones,
 109 this is likely due to the conductance from Cl⁻ ions remnant which are more available at lower
 110 annealing temperature. Although 300 °C annealing should improve crystallinity of the h-ZnO flakes
 111 ⁸⁻⁹, with less dopant available in the band gap potentially lowers the conductance given the improved
 112 crystallinity. This becomes evident in 0.5M case where Cl⁻ ions become more dominant prior to

113 growth but are later eliminated when annealed at higher temperature potentially resulting in more
114 defective channel when used as source and drain contacts.

115

116 **References for Supplementary Materials**

117

118 1. Choopun, S.; Hongsith, N.; Wongrat, E., Metal-Oxide Nanowires by Thermal Oxidation Reaction
119 Technique. **2010**.

120 2. Wu, Z.; Yang, S.; Wu, W., Shape control of inorganic nanoparticles from solution. *Nanoscale* **2016**,
121 *8* (3), 1237-59.

122 3. Vega-Poot, A. G.; Rodriguez-Gattorno, G.; Soberanis-Dominguez, O. E.; Patino-Diaz, R. T.;
123 Espinosa-Pesqueira, M.; Oskam, G., The nucleation kinetics of ZnO nanoparticles from ZnCl₂ in
124 ethanol solutions. *Nanoscale* **2010**, *2* (12), 2710-7.

125 4. Wang, Z. L., Zinc oxide nanostructures: growth, properties and applications. *Journal of Physics:*
126 *Condensed Matter* **2004**, *16* (25), R829-R858.

127 5. Thanh, N. T.; Maclean, N.; Mahiddine, S., Mechanisms of nucleation and growth of nanoparticles
128 in solution. *Chem Rev* **2014**, *114* (15), 7610-30.

129 6. Lizandara-Pueyo, C.; van den Berg, M. W. E.; De Toni, A.; Goes, T.; Polarz, S., Nucleation and
130 Growth of ZnO in Organic Solvents - an in Situ Study. *Journal of the American Chemical Society* **2008**,
131 *130* (49), 16601-16610.

132 7. Kim, J.; Kim, G.; Kyun Kim, T.; Kwon, S.; Back, H.; Lee, J.; Ho Lee, S.; Kang, H.; Lee, K., Efficient
133 planar-heterojunction perovskite solar cells achieved via interfacial modification of a sol-gel ZnO
134 electron collection layer. *Journal of Materials Chemistry A* **2014**, *2* (41), 17291-17296.

135 8. Gao, X.-D.; Li, X.-M.; Zhang, S.; Yu, W.-D.; Qiu, J.-J., ZnO submicron structures of controlled
136 morphology synthesized in zinc-hexamethylenetetramine-ethylenediamine aqueous system. *Journal*
137 *of Materials Research* **2011**, *22* (07), 1815-1823.

138 9. Park, S.; An, S.; Ko, H.; Jin, C.; Lee, C., Synthesis of Nanograined ZnO Nanowires and Their
139 Enhanced Gas Sensing Properties. *ACS Appl. Mater. Interfaces* **2012**, *4* (7), 3650-3656.

140